

SUPPLEMENTARY INFORMATION

FOR

Growth amplification in ultrahigh-throughput microdroplet screening increases sensitivity of clonal enzyme assays and minimizes phenotypic variation

Paul Jannis Zurek,^{a,b} Raphaëlle Hours,^{a,b} Ursula Schell,^b Ahir Pushpanath^b and Florian Hollfelder^{*a}

^aDepartment of Biochemistry, University of Cambridge, 80 Tennis Court Road, CB2 1GA Cambridge, United Kingdom

^bJohnson Matthey Plc, 260 Cambridge Science Park, CB4 0WE Cambridge, United Kingdom

*Corresponding author: fh111@cam.ac.uk

1. Droplet incubation chambers from conventional reaction tubes

In the experiments described in this work droplet emulsions were generally stored in incubation chambers (Fig. S1). Incubation chambers were also used to hold the emulsion during oxygenation for cell growth. To prepare these chambers, access holes were opened with a 1 mm biopsy punch at the side and at the tip of a conventional 0.5 ml plastic reaction tube. The reaction tube was glued with its lid on a 1-mm thick microscopy glass slide for stability. Polyethylene tubing (0.38 mm inner diameter, 1.09 mm outer diameter, Smiths Medical) was inserted in the access holes. Tubing was fixed in place with a high viscosity cyanoacrylate glue (Scotch-Weld PR1500) and allowed to dry overnight. To collect droplets in the incubation chamber, the chamber was first filled with oil (HFE-7500 (3M Novec) with 1% 008-FluoroSurfactant (RAN Biotechnologies)) from a syringe. Removing the syringe again and leveraging the side access tubing height resulted in the oil slowly flowing out of the chamber from the top access. Now, the top access tubing was connected to the outlet of a droplet generation chip to collect the emulsion in the chamber without introducing air. Droplets can now enter from the top and pack in the chamber, while excess oil from generation is flowing out of the open side access tubing. At the end of collection, the chamber was disconnected from the droplet generation chip and an oil-filled syringe was connected to the side access tubing to close the system. To eject droplets after incubation, e.g. to introduce the emulsion to the sorting chip, the emulsion was pushed out with the oil-filled syringe connected to the side access tubing.

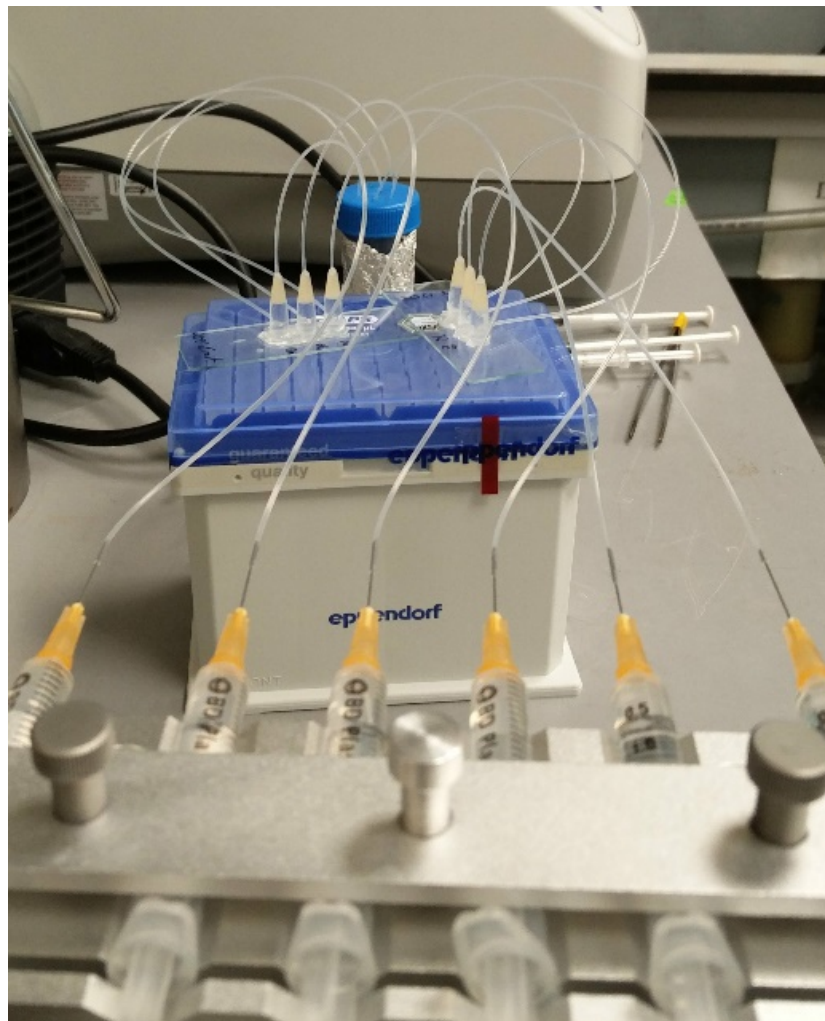


Fig. S1: Multiple droplet incubation chambers during oxygenation for cell growth in droplets.

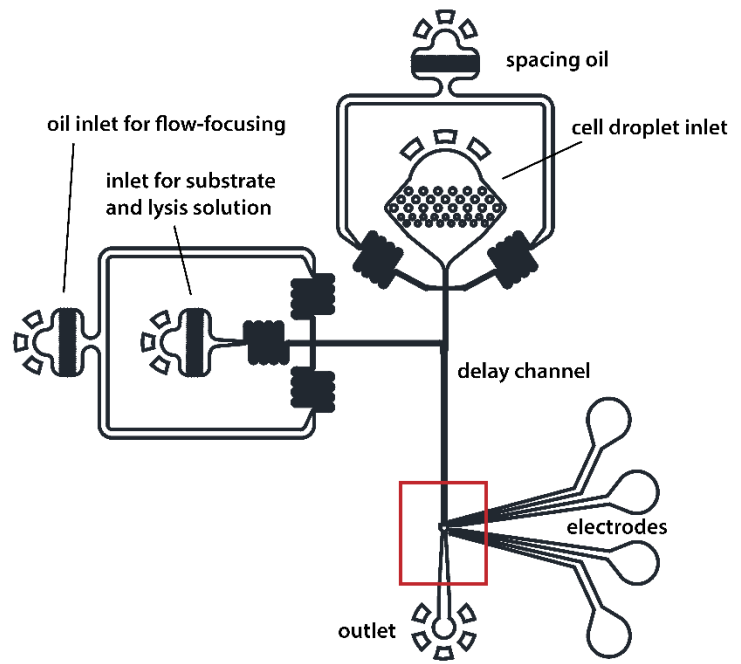
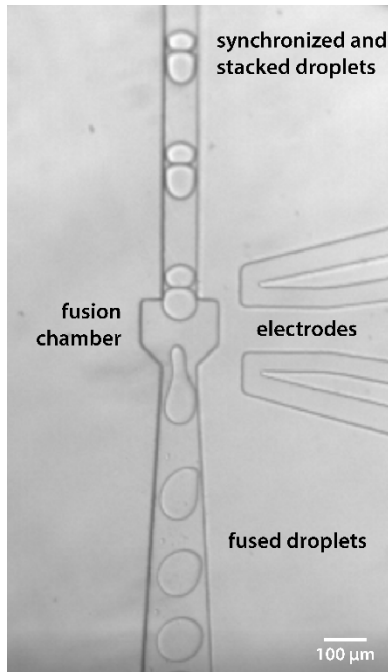


Fig. S2: *Left:* Picture of the pico-fusion chip used in this work in operation. Stacked droplets enter the fusion chamber, where an electric field is applied to cause droplet coalescence. *Right:* Schematic drawing of the pico-fusion chip. The view seen in the left image is marked here as a red box.

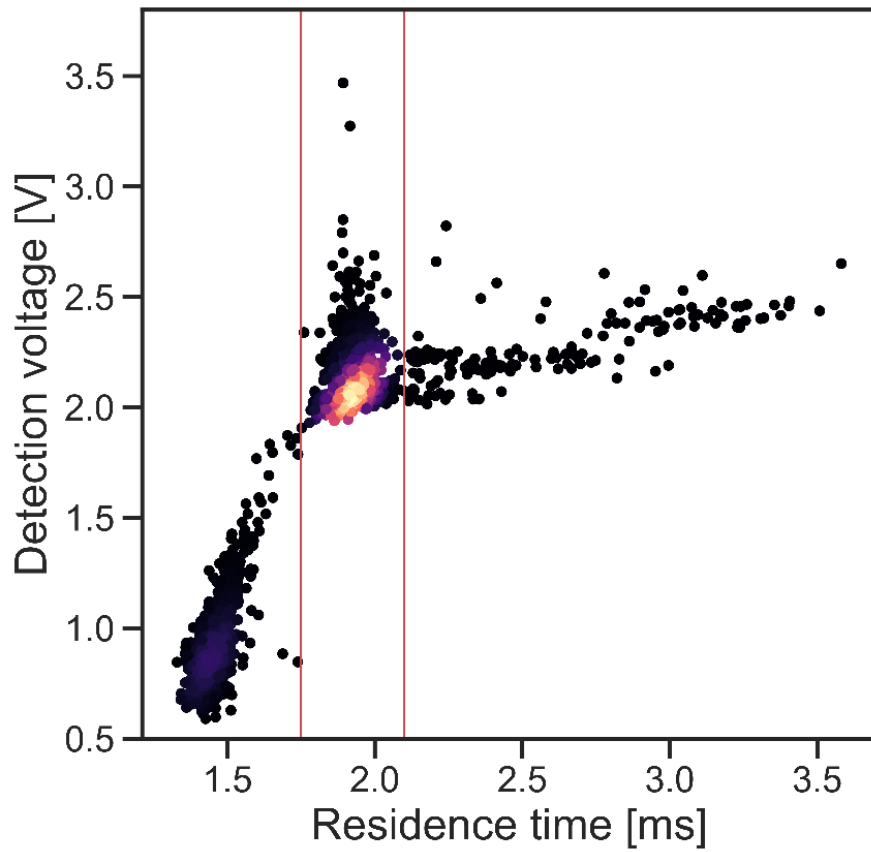


Fig. S3: Size, expressed as residence time, and absorbance of 5000 droplets, measured in the cell growth workflow (as in Fig. 4C). The size gate applied to sorting is marked in red, to exclude smaller non-fused droplet and larger erroneous fusions. The big main population represents empty droplets or inactive variants, showing a tail of active AmDH variants.

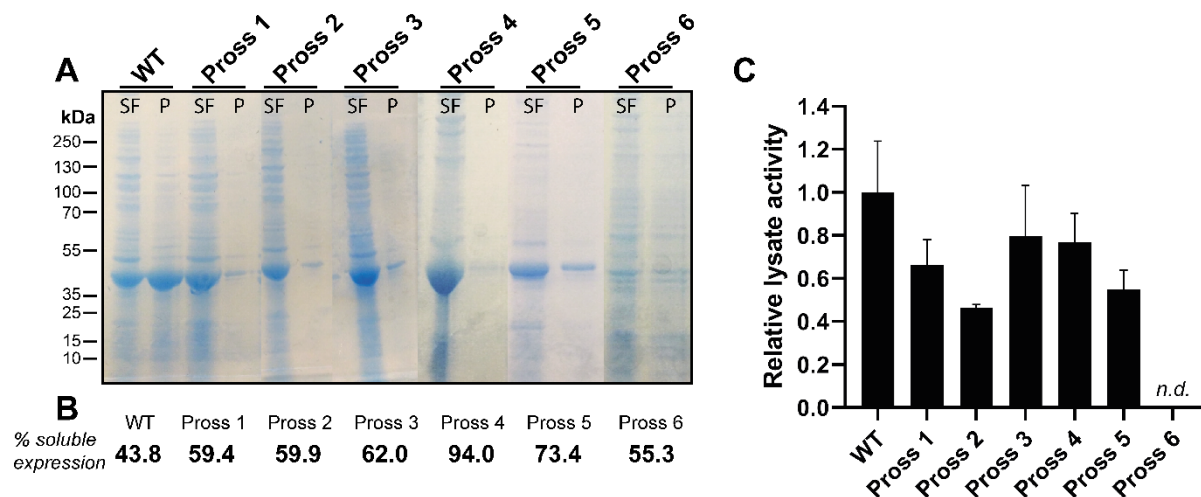


Fig. S4: Expression levels and activities in cell lysate of the six stabilized AADH variants, computationally designed using the Pross algorithm.¹ After computational predictions starting with the WT AADH (PDB ID 1C1D, UniProt ID Q59771) without additional stabilizing features, the genes of the six variants Pross 1 to 6 were synthesized. The corresponding plasmids were then transformed into *E. coli* and expressed overnight at 20 °C. **A:** Soluble expression levels of protein variants. After protein expression, the soluble and insoluble fractions of cell lysates were analysed by SDS-PAGE. SF: soluble fraction, P: pellet. **B:** Soluble expression levels quantified by densitometric analysis of the gel images (shown in A). **C:** The activity of each variant in cell lysate was determined relative to that of WT AADH. The plot shows averages of triplicates in three independent measurements, with error bars representing ± 1 SD. *Conditions:* glycine-KOH buffer = 100 mM, pH 10, T = 20 °C, with 10 mM L-Phenylalanine and 10 mM NAD⁺. Finally, the fourth design (Pross 4, see below for sequence) was chosen for further experiments as AADH^{mut} and turned into an AmDH, as it showed the highest soluble expression at good lysate activities.

2. Improved Arduino sorting algorithm

The script for the Arduino Due microcontroller that actuates sorting electronics was improved. Previously, the Arduino would run a simple point-over-threshold script, triggering and sorting droplets as soon as the absorbance reached a fixed threshold. The new script, as outlined below, enables 2D sorting by detecting signal peak and duration. Detection is based on the highest value within an event, enabling sorting of low absorbent populations. Also, the signal width is measured as an approximation for droplet size.

```
/*
ABSORBANCE SORTING SCRIPT for 2D sorting gates
*/

//Sorting variables
float thresh = 8.0;           //set to voltage ~0.5 below baseline
float sortVH = 5.0;          //set to high voltage limit for selection
float sortVL = 0.0;          //set to low voltage limit for selection
unsigned long peakWH = 2000UL; //set to high size gate (in us) for selection
unsigned long peakWL = 500UL; //set to low size gate (in us) for selection
unsigned long minDist = 1000UL; //min distance to last peak to exclude doublets

//Electrode timing
int electrode_delay = 250;    //Pulse delay in us
int electrode_pulse = 5;      //Pulse width in ms

void setup() {
  pinMode(13, OUTPUT);
  digitalWrite(13, LOW);
  REG_ADC_MR = (REG_ADC_MR & 0xFFFF0FFF) | 0x00020000;
  Serial.begin(115200);
  analogReadResolution(12);
}

//Read and convert the detector voltage
float readout() {
  int sensorValue = analogRead(A0);
  float result = sensorValue / 4096.0 * 10;    //Scale to 0-10V
  return result;
}

//loop variables
float v = 10.0;
float vo = 10.0;
float peakV = 10.0;
unsigned long t1 = 0UL;
unsigned long t2 = 0UL;
unsigned long tlast = 0UL;

void loop() {
  vo = v;
  v = readout();    //get signal from detector and convert

  if ((vo > thresh) and (v < thresh)) { //left event border
    t1 = micros();
  }

  if ((vo < thresh) and (v > thresh)) { //right event border
    tlast = t2;
    t2 = micros();
  }

  //check size
  if (((t1-tlast) > minDist) && ((t2-t1) > peakWL) && ((t2-t1) < peakWH)) {
    //check voltage
```

```
    if ((peakV > sortVL) && (peakV < sortVH)) {
        delayMicroseconds(electrode_delay);
        digitalWrite(13, HIGH);
        delay(electrode_pulse);
        digitalWrite(13, LOW);
    }
}

//Below thresh control
if (v < thresh) {
    if (v < peakV) {
        peakV = v;
    }
}
//Above thresh control
if (v > thresh) {
    peakV = 10.0;
}
}
```

3. Amino Acid Sequence of the PheDH mutant Pross 4

This variant was generated by the Pross algorithm¹ to increase protein stability. Mutations introduced to the parent WT AADH (UniProt ID Q59771) are highlighted.

>PheDH_PROSS-stabilized_design-4

```
MSIDSALNWDGEMTVTRFDAAATGAHFVIRIHSSTQLGPAAGGTRAWQYSSWADALTDAGRLARAMTYKM  
AVAGLPMGGGKSVIALPAPRHSIDPSTWARILRAHAEMIDSLNGRYWTGPDVNTNSADMIDILADETEF  
VFGRSPERGGAGSSAFTTALGVFEAMKATVAHRGLGSLDGLTVLVQGLGAVGGSLAKLLAEAGAQLLV  
ADTDTERVALAVELGHTWVALDDVLSTPCDVFAPCAMGGVITDEVARTLDCKVVCGAANNVLAHEAAA  
DILHARGILYAPDFVANAGGAIHLVGREVLGWSEDOVHERARAIGDTLKEVFEIADKDGVTPEAARE  
LAERRMREASTTTATA
```

4. Supplementary References

- 1 A. Goldenzweig, M. Goldsmith, S. E. Hill, O. Gertman, P. Laurino, Y. Ashani, O. Dym, T. Unger, S. Albeck, J. Prilusky, R. L. Lieberman, A. Aharoni, I. Silman, J. L. Sussman, D. S. Tawfik and S. J. Fleishman, *Mol. Cell*, 2016, **63**, 337–346.